

On the hadronic γ -ray emission from Tycho’s Supernova Remnant

Xiao Zhang,¹ Yang Chen,^{1,2,*} Hui Li¹ and Xin Zhou^{3,2,4}

¹*Department of Astronomy, Nanjing University, Nanjing 210093, P. R. China*

²*Key Laboratory of Modern Astronomy and Astrophysics, Nanjing University, Ministry of Education, China*

³*Purple Mountain Observatory, 2 West Beijing Road, Nanjing 210008, China*

⁴*Key Laboratory of Radio Astronomy, Chinese Academy of Sciences, Nanjing 210008, China*

ABSTRACT

Hadronic γ -ray emission from supernova remnants (SNRs) is an important tool to test shock acceleration of cosmic ray protons. Tycho is one of nearly a dozen Galactic SNRs which are suggested to emit hadronic γ -ray emission. Among them, however, it is the only one in which the hadronic emission is proposed to arise from the interaction with low-density ($\sim 0.3 \text{ cm}^{-3}$) ambient medium. Here we present an alternative hadronic explanation with a modest conversion efficiency (of order 1%) for this young remnant. With such an efficiency, a normal electron-proton ratio (of order 10^{-2}) is derived from the radio and X-ray synchrotron spectra and an average ambient density that is at least one-order-of-magnitude higher is derived from the hadronic γ -ray flux. This result is consistent with the multi-band evidence of the presence of dense medium from the north to the east of the Tycho SNR. The SNR-cloud association, in combination with the HI absorption data, helps to constrain the so-far controversial distance to Tycho and leads to an estimate of 2.5 kpc.

Key words: γ -rays: theory – ISM: individual (Tycho) – radiation mechanisms: non-thermal

1 INTRODUCTION

Energetic cosmic rays (CRs) below the “knee” energy $\sim 3 \times 10^{15}$ eV are usually believed to be accelerated in shock waves of Galactic SNRs through the diffusive shock acceleration (DSA). Moreover, it has been commonly assumed that some 10% of the explosion energy of a supernova is transferred to CRs throughout its whole life in order to explain the observational CR energy density in our Galaxy (e.g., Baade & Zwicky 1934; Ginzburg & Syrovatskij 1967). The theory of DSA of cosmic rays is well established (see e.g., Malkov & O’C Drury 2001, for reviews, and references therein), but there is no direct evidence for such acceleration of the CR protons, and the energy conversion efficiency, the fraction of the explosion energy converted to CR energy, still remain elusive.

An important clue comes from the hadronic γ -ray emission from the neutral pion decay which ensues from the collision of the accelerated protons with the baryons in proximate dense matter. It is, however, even difficult to distinguish the hadronic γ -ray emission from the leptonic emis-

sion, and thus the environmental effect on the γ -ray emission is very noteworthy. So far, γ -rays from some SNRs have been interpreted to arise from hadronic processes, such as W28, W41, W44, W49B, W51C, Cygnus Loop, IC443, CTB 37A, and G349.7+0.2 (see Li & Chen 2012, and references therein). The γ -rays from the Cas A SNR are also explained to have a hadronic contribution at the GeV energy range at least (Araya & Cui 2010). The hadronic γ -rays from these SNRs are all suggested to be emitted by the interaction with dense matter. For the γ -ray emission from the Tycho SNR, as a contrast, the hadronic scenario invokes a tenuous ambient medium (e.g., Giordano et al., 2012; Tang, Fang & Zhang 2011; Morlino & Caprioli 2012).

Tycho’s SNR (G120.1+01.4; 3C 10; SN 1572) is the historical relic of a Type Ia supernova as verified with the light echo from the explosion (Krause et al. 2008). As one of the few accurately known-age SNRs, Tycho’s SNR has been well studied over the entire spectrum. It shows a shell-like morphology in radio with enhanced emission along the north-eastern edge (e.g., Dickel et al. 1991), and has spectral index of 0.65 and a flux density of 40.5 Jy at 1.4 GHz (Kotthes et al. 2006). Strong non-thermal X-ray emission is concentrated in the SNR rim, forming a thin filamentary structure (e.g.,

* E-mail: ygchen@nju.edu.cn

Hwang et al. 2002; Bamba et al. 2005; Warren et al. 2005). Recently, TeV and GeV γ -ray emission was successively detected from this SNR (Acciari et al. 2011; Giordano et al. 2012) and thus provides a new opportunity for studying particle acceleration in SNRs and high energy non-thermal radiation. Taking the multi-band spectrum into account, it has been shown that the hadronic process, with energy conversion efficiency of 10–15% for the current stage, naturally explains the GeV–TeV γ -ray emission (Giordano et al. 2012; Tang et al. 2011; Morlino & Caprioli 2012), although it is argued that a two-zone leptonic model can also work (Atoyan & Dermer 2012). In the hadronic scenario, the target gas is always suggested to be a low-density ambient interstellar medium ($n_{\text{H}} \sim 0.2\text{--}0.3 \text{ cm}^{-3}$), which is quite different from the case of the aforesaid SNRs.

Although it is suggested that Tycho is a naked Ia SNR without any dense clouds (Tian & Leahy 2011), there seem to be signs and evidence in multiband showing the presence of dense clouds from the north to the east (see a summary in §3.1), which could be the target for bombardment of the accelerated protons and would thus reduce the needed converted energy. While, theoretically, the acceleration efficiency in SNRs is not well determined, very efficient acceleration process has been suggested (e.g., Helder et al. 2009), and some self-consistent models predict that the converted energy fraction can be up to $\sim 60\% - 80\%$ in the whole lifetime of an SNR (e.g., Berezhko & Völk 1997; Kang & Jones 2006). However, constraints from some γ -ray bright young Galactic SNRs hint that the fraction would not be greater than 10% at Tycho’s age but could reach 10–20% in subsequent 1–2 kyr, such as the case of RX J1713.7-3946 (e.g., Lee et al. 2012). The similarly young SNR Cas A has only transferred a minor fraction ($\lesssim 2\%$) of the total kinetic energy to accelerated particles (Abdo et al. 2010; Araya & Cui 2010). Moreover, under the Bohm limit assumption, the conversion factor no more than 1.3 % is predicted in kinetic models for a SNR at the Tycho’s age, evolving in a pre-shock medium of density $\sim 0.3 \text{ cm}^{-3}$, although its total conversion fraction can be more than 60% (e.g., Berezhko & Völk 1997). Therefore, the fraction of order $\sim 1\%$ at Tycho’s age deserves serious consideration.

Here we present an alternative hadronic scenario with the modest energy conversion fraction of order $\sim 1\%$ for the present Tycho SNR. As shown below, with such a reduced energy fraction, not only the normal number ratio between the accelerated electrons and protons is obtained, but also the gas density in the region of hadronic process will be increased by one order of magnitude, consistent with the presence of (at least local) dense medium, e.g. molecular clouds (MCs). If this is true, the Tycho’s SNR will be the only Type Ia SNR associated with MCs among the currently known interacting SNRs (Jiang et al. 2010).

2 HADRONIC GAMMA-RAY EMISSION

We assume that the spectrum of the shock-accelerated particles (electrons and protons) obeys a power law with an energy cutoff:

$$dN_i/dE_i = A_i E_i^{-\alpha_i} \times \exp(-E_i/E_{i,\text{cut}}) \quad (1)$$

where $i = e, p$, E_i is the particle kinetic energy, α_i is the spectral index and is fixed as $\alpha_{e,p} \simeq 2.3$ according to the afore-mentioned radio index and the charge-independent acceleration process, $E_{i,\text{cut}}$ is the cut-off energy and, for protons, can be taken as $E_{p,\text{max}} \simeq (37 \text{ TeV})(B_d/100 \mu\text{G})^2$ (Parizot et al. 2006) while $E_{e,\text{cut}}$ is confined by radiative limit, and A_i is normalization factor and can be determined from $\eta E_{\text{SN}} = \int_{m_e c^2}^{\infty} A_e E_e^{-\alpha_e} \times \exp(-E_e/E_{e,\text{cut}}) E_e dE_e + \int_{m_p c^2}^{\infty} A_p E_p^{-\alpha_p} \times \exp(-E_p/E_{p,\text{cut}}) E_p dE_p$ combined with adjustable parameter, $K_{ep} = A_e/A_p$, the number ratio between the accelerated electrons and protons at a given energy. Here the energy conversion efficiency $\eta \sim 1\%$ is adopted, and E_{SN} is the explosion energy of Tycho. According to the estimate from the expansion rate of the X-ray emitting ejecta (Hughes 2000), we will adopt $E_{\text{SN}} = 6 \times 10^{50} d_{2.5}^2 \text{ erg}$, where $d_{2.5}$ is the distance to the SNR scaled with 2.5 kpc, in view of the physical contact of Tycho with interstellar dense clouds (see §3).

For the γ -ray emission, we consider three potential radiation processes: inverse-Compton (IC) scattering on the cosmic microwave background by relativistic electrons, non-thermal bremsstrahlung by relativistic electrons (using the differential cross sections given in Baring et al. 1999), and π^0 -decay γ -rays resulting from p-p interaction (Kelner et al. 2006, using the parametrization therein).

The downstream magnetic field strength is estimated by X-ray measurements and is listed as a function of the distance to this SNR (Cassam-Chenaï et al. 2007, Table 5 therein). Since in this letter we favor an association of Tycho with dense clouds at a distance of 2.5 kpc (see §3.3), the field strength can be estimated as $B_d \simeq 320 \mu\text{G}$ by interpolation. This number is also consistent with the estimates (around $300 \mu\text{G}$) given by other methods (Völk et al. 2005; Morlino & Caprioli 2012).

From the radio and X-ray synchrotron spectral data and the assumed energy conversion efficiency, we get $E_{e,\text{cut}} \approx 5.6 \text{ TeV}$ and $K_{ep} \approx 0.7 \times 10^{-2}$. Actually, the product ηK_{ep} is a constant, with the synchrotron flux given (shown in Figure 1); by contrast, the cases using an efficiency $\sim 10\%$ correspond to a K_{ep} value $\lesssim 10^{-3}$ (e.g., Morlino & Caprioli 2012; Giordano et al. 2012). Recently a lower limit for the electron to proton ratio, $K_{ep} \gtrsim 10^{-3}$, is implied by the radio observations of SNRs in nearby galaxies (Katz & Waxman 2008). Actually, K_{ep} of order $\sim 10^{-2}$ is commonly favoured based on the measured electron to proton ratio in the CRs under the assumption that SNRs are the main source of proton and electron CRs (see e.g., Longair 1994; Katz & Waxman 2008).

By fitting γ -ray spectrum, which is here considered to be due to hadronic emission (see Figure 2), and approximating the total energy of the relativistic protons to be ηE_{SN} , we obtain the product of η and the average density (averaged over the entire shock surface) of the target protons (with which the energetic particles interact), n_t , and this product is shown as a $n_t - \eta$ line in Figure 1. We have $n_t \sim 12 \text{ cm}^{-3}$ for $\eta \sim 1\%$. The target protons can be located both upstream and downstream, since the accelerated particles move back and forth. Downstream, the average compression factor is estimated to be around 3 (Giordano et al. 2012). Thus the average preshock target proton density, n_0 , is in the range $\sim 4\text{--}12 \text{ cm}^{-3}$. This density value is much

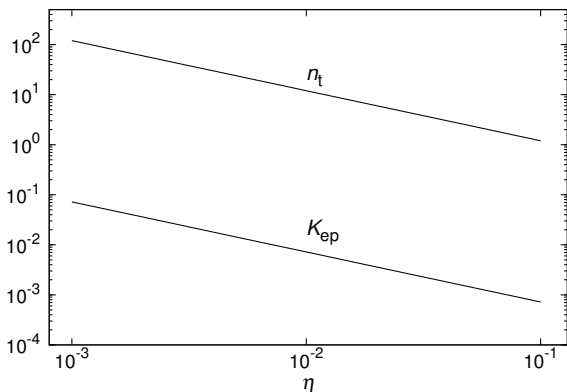


Figure 1. Dependence of the parameters, K_{ep} and n_t , on the energy conversion efficiency η .

larger than the gas density ($n_{\text{H}} \sim 0.3 \text{ cm}^{-3}$), over an order of magnitude, estimated from the previous optical measurement for the northeast (NE) filament (Kirshner et al. 1987) and the *Chandra* X-ray observations (Cassam-Chenaï et al. 2007; Katsuda et al. 2010). In §3.2, we will explain such discrepancy in density for the SNR shock (as in the NE) expanding in an environment with MCs.

In the above calculation, the diffusive process of the shock accelerated CRs is not considered. Actually, the typical diffusion radius of CRs around SNRs is $R_{\text{dif}} = 2\sqrt{D(E)t_{\text{dif}}} \approx 0.76 (t_{\text{dif}}/440 \text{ yr})^{0.5} \text{ pc}$ for 10 GeV protons (here the correction factor of slow diffusion around the SNR, $\chi \sim 0.01$, has been adopted, see e.g., Fujita et al. 2009; Giuliani et al. 2010; Gabici et al. 2010; Li & Chen 2012). Since the diffusion time scale t_{dif} can not be larger than the SNR's age 440 yr, the diffusion distance for the protons with energy 10 GeV, which are responsible for $\sim 1 \text{ GeV}$ γ -rays, is smaller than 0.8 pc and significantly smaller than the SNR's radius $\simeq 3 d_{2.5} \text{ pc}$. Therefore, in the young SNR Tycho, the hadronic emission does not primarily arise from the CR protons which collide nearby molecular gas after a long time diffusion, as in the cases of several interacting SNRs that are considerably older ($\geq 2 \text{ kyr}$, see e.g., Li & Chen 2012).

3 PHYSICAL CONTACT WITH DENSE CLOUDS AND THE DISTANCE

3.1 The evidence of shock-cloud interaction

In the previous section, it is shown that a dense ambient medium ($n_0 \sim 4 - 12 \text{ cm}^{-3}$ on average) is inferred, much denser than the preshock gas that was previously derived ($\sim 0.3 \text{ cm}^{-3}$). A dense ambient density (3 cm^{-3}) was also suggested by a recent hydrodynamic simulation (Badenes et al. 2007). Indeed, dense medium (molecular gas in particular) has been suggested to be present in the surroundings of the SNR from the north to the east based on multi-band observational evidence.

The first evidence comes from the reduced expansion rate of the SNR in the NE compared to other peripheral parts. Radio (Reynoso et al. 1997) and X-ray (Hughes 2000; Katsuda et al. 2010) observations show that, along the pe-

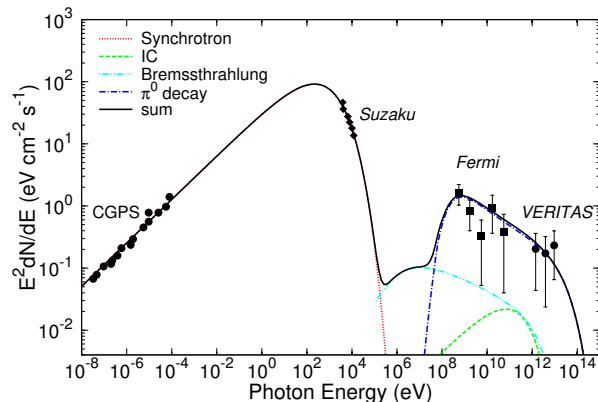


Figure 2. Broadband SED of Tycho's SNR with the observed data in radio (Kotthes et al. 2006), X-rays (Tamagawa et al. 2009) and γ -rays (*Fermi*: Giordano et al. 2012; *VERITAS*: Acciari et al. 2011).

riphery of the remnant, although the northeastern section has the largest radius, its expansion index is smaller than that in all the remaining parts. Such evidence suggests that the northeastern peripheral gas currently is moving the slowest and being remarkably decelerated and that the gas density in the NE is significantly higher than that in other parts. It is suggested that the shock front in the NE has reached the outskirts of dense clouds in the recent past (Reynoso et al. 1999). In addition, the fact that this slowest expansion part has the flattest spectral index 0.44 ± 0.02 (Katz-Stone et al. 2000) might be another indication for the interaction with MCs (Koo et al. 2001). Similar phenomenon also appears in the interacting regions of other SNRs, such as W28 (Dubner et al. 2000) and IC443 (Green 1986).

Secondly, there seem to be some direct signs of the presence of adjacent dense clouds from the CO line observations. The ^{12}CO ($J=1-0$) observations show that the MCs at $-68 \text{ km s}^{-1} \leq V_{\text{LSR}} \leq -58 \text{ km s}^{-1}$ forms a semi-closed non-uniform large shell surrounding the SNR from the north to the east and the inner boundary essentially traces the rim of Tycho (Lee, Koo & Tatematsu 2004; Cai, Yang & Lu 2009). A high-resolution ($16''$) close-up observation shows that the $-63.5 \text{ km s}^{-1} \leq V_{\text{LSR}} \leq -61.5 \text{ km s}^{-1}$ ^{12}CO ($J=1-0$) emitting area appears to be in contact with the remnant along its northeastern boundary (Lee et al. 2004). Specifically, there is a big molecular clump in the integration map of this velocity component (see Fig. 1 in Lee et al. 2004) at the azimuth corresponding to the slowest expansion (Reynoso et al. 1997). A similar emitting zone at $\sim -62.5 \text{ km s}^{-1}$ is also revealed by the submillimeter observation in the higher level transition line, ^{12}CO ($J=2-1$) (Xu, Wang & Miller 2011). The virial mass of the surrounding MCs derived from the ^{12}CO ($J=1-0$) emission is found to be larger than their gravitational mass, implying that the MCs are being violently disturbed and Tycho's shock is very likely to be responsible for the disturbance (Cai et al. 2009). Such disturbance seems to be consistent with the broad ^{12}CO ($J=2-1$) lines present in -68 to -55 km s^{-1} interval for a few adjacent MCs (Xu et al. 2011).

Thirdly, interaction with dense medium is also favoured

by the far- to mid-IR observations (Ishihara et al. 2010; Gomez et al. 2012). The far-IR emissions (*AKARI*: 140 and 160 μm ; *Herschel*: 160, 250, 350 and 500 μm), which originate from cold dust, are spatially correspondent to the CO emission in -68 to -53 km s^{-1} interval. The mid-IR emissions (*AKARI*: 15, 18, and 24 μm ; *Herschel*: 24 and 70 μm), which primarily shows warm dust distribution, reveal a shell-like emission structure along the remnant boundary except in the west and southwest and seem to delineate the interface between the remnant and the MCs. They have been pointed out to arise from the outer edge of the shock heated cold dust and MCs, although the possibility that a small fraction of the warm dust was formed in the supernova ejecta was not absolutely ruled out (Ishihara et al. 2010; Gomez et al. 2012). The mid-IR filter bands, such as *AKARI* L15 (12.6–19.4 μm) and L18W (13.9–25.6 μm), may also include the contribution from the rotational lines of hydrogen molecules (like S(1) $J = 3-1$ at 17.03 μm ; Ishihara et al. 2010). As an alternative, the mid-IR emissions are suggested to come from the swept-up interstellar dust through interaction with the HI clump in the NE, shown as a significant absorption feature in the -52.7 km s^{-1} , which is also at the azimuthal range of the slowest expansion and the faint overlapping -55 km s^{-1} MC in the NW (Gomez et al. 2012).

3.2 Discussion about the shock in cloudy medium

The presence of dense clouds along the boundary, especially in the NE, and the large target-particle density derived here can be compatible with the low density preshock gas that is previously inferred from optical and X-ray observations. Here we mention two possible cases for the shock-cloud interaction.

The first case is that the blast shock may be flanking a cloud (e.g. the slowed-expansion portion in the NE) and the shocked gas outside the cloud (but along the line of sight) has a density of order 0.1 cm^{-3} as observed in X-rays and optical. The solid angle fraction of the whole remnant covered by the interacting region may roughly be $f_{\Omega} \sim 0.07$, where a subtended angle $\sim 60^{\circ}$ is adopted from the slowed-expansion portion (Reynoso et al. 1997). The molecular gas surrounding Tycho may have a density n_{MC} as high as $\sim 10^2 \text{ cm}^{-3}$ (Tian & Leahy 2011). Thus the average preshock proton density is $n_0 = f_{\Omega}(2n_{\text{MC}}) \sim 14(n_{\text{MC}}/100 \text{ cm}^{-3}) \text{ cm}^{-3}$, which is very similar to the value we obtain above (considering the uncertainties in the used parameters).

The alternative case is that the shock may be expanding into a clumpy medium and the low density corresponds to the interclump medium that fills in most of the volume. For instance, blast shocks are found to propagate into the interclump gas of densities of order 0.1 cm^{-3} in the southeastern edge of Kes 69 (Zhou et al. 2009) and in the northeastern edge of Kes 78 (Zhou & Chen 2011), where the shocks are interacting with MCs, as derived from the X-ray analyses; in W28, W44, and 3C 391, where blast waves are impacting MCs, the preshock density of the interclump gas is also $< 1 \text{ cm}^{-3}$ as inferred from the IR spectroscopic study (Reach & Rho 2000). If $n_0 \sim 4-12 \text{ cm}^{-3}$ derived above from the hadronic emission is used and the clump filling factor in the dense cloud is denoted as f_c (which may be of order 0.1 or smaller), then the solid angle fraction covered by the cloud(s) is $f_{\Omega} = n_0/(2n_{\text{MC}}f_c) \sim 0.2-$

$0.6(n_{\text{MC}}/100 \text{ cm}^{-3})^{-1}(f_c/0.1)^{-1}$. Such a solid angle seems to be consistent with the distribution of semi-closed dense gas surrounding the SNR as suggested by the CO line and IR observations (§3.1).

We note that there is not yet report of detection of optical emission from the shocked clouds. One of the possibilities may be that the shock collision with the clouds is a very recent event, e.g., within 50 yr (Reynoso et al. 1999), which is shorter than the radiative cooling time $\sim 300 \text{ yr}$ (using Eq.(3) in Sgro 1975, with the velocity of the blast shock $0.3'' \text{ yr}^{-1}$ at 2.5 kpc or 3500 km s^{-1} adopted). Little thermal X-rays are either detected from the shocked clouds. A similar case is seen in RX J1713.7-3946, another young SNR interacting with MCs (Moriguchi et al. 2005). It is pointed out that the substantial suppression of the thermal X-ray emission could result from the very low intercloud gas density and the stall of the transmitted shock in the clouds (Zirakashvili & Aharonian 2010; Inoue et al. 2012).

3.3 Distance to Tycho

The SNR-cloud association, in combination with the line-of-sight HI absorption (Tian & Leahy 2011), can be used to estimate the distance to the Tycho’s SNR, which has long been in debate due to its special location in our Galaxy (see a brief summary in Figure 6 of Hayato et al. 2010). The LSR velocity $\sim -62 \text{ km s}^{-1}$ of the semi-closed molecular shell (including the northeastern MCs) allows two alternatives for the distance, 4.6 kpc and 2.5 kpc, while the LSR velocity $\sim -55 \text{ km s}^{-1}$ of the faint northwestern MC allows 4.0 kpc and 2.5 kpc. The latter estimates are because of the deep “dip” at 2.5 kpc, where the spiral shock front is located, in the rotation curve for the longitude 120° (Tian & Leahy 2011; using the Foster & MacWilliams’ (2006) model; also see Figure 14 of Schwarz et al. 1995) and the b -dependent behaviour of the velocity field in the spiral shock region, in which the systematic velocity of the MCs could be as low as $\lesssim -60 \text{ km s}^{-1}$ (Lee et al. 2004). Due to the absence of the absorption feature for the HI gas at -41 to -46 km s^{-1} , Tycho should be in front of this gas, as Tian & Leahy (2011) constraint it to be nearer than 3 kpc, and thus the alternative distances of 4.6 kpc and 4.0 kpc are excluded. In the scenario of the association with the $\sim -62 \text{ km s}^{-1}$ velocity component, the HI gas $\sim -60 \text{ km s}^{-1}$ (lack of absorption feature, Tian & Leahy 2011) is behind the SNR, and the -47 to -53 km s^{-1} HI absorbing gas is in the front, but all of them are closely around the spiral shock at the “dip”, at the distance of 2.5 kpc. In the scenario of the association between the remnant and the $\sim -55 \text{ km s}^{-1}$ MC and the -52.7 km s^{-1} HI cloud (see §3.1), the situation of HI absorption and SNR location is similar. Tycho is located in the high density region just behind the spiral shock (Lee et al. 2004) and is now encountering the inhomogeneous outskirts of the $\sim -62 \text{ km s}^{-1}$ or/and $\sim -55 \text{ km s}^{-1}$ MCs.

4 CONCLUSION

Tycho is one of nearly a dozen Galactic SNRs which are suggested to radiate hadronic γ -ray emission. It is noted, however, that it is the only one in which the hadronic emission is proposed to arise from the interaction with low-density

($\sim 0.3 \text{ cm}^{-3}$) ambient medium. An alternative explanation that the γ -rays originate from hadronic process with fewer energetic protons but denser target gas is presented here. With a conversion efficiency of order 1% for this young historical SNR, a normal electron-proton ratio (of order 10^{-2}) is derived from the radio and X-ray synchrotron spectra and an average ambient density that is at least one-order-of-magnitude higher is further derived from the hadronic γ -ray flux. This result is consistent with the multi-band observational evidence of the presence of the surrounding dense medium from the north to the east. The interaction scenario, combined with the HI absorption data, is used to constrain the long controversial problem of the distance to Tycho and leads to an estimate of 2.5 kpc.

ACKNOWLEDGMENTS

The anonymous referee is acknowledged for valuable comments and advices, which have helped to improve the manuscript. We thank Wenwu Tian, Siming Liu, Daisuke Ishihara and Ping Zhou for helpful advices. Y.C. acknowledges support from the 973 Program grant 2009CB824800 and NSFC grants 11233001 and 10725312. X.Z. thanks support from the China Postdoctoral Science Foundation grant 2011M500963.

REFERENCES

- Abdo A. A. et al., 2010, *ApJ*, 710, L92
 Acciari V. A. et al., 2011, *ApJ*, 730, L20
 Araya M., Cui W., 2010, *ApJ*, 720, 20
 Atoyan A., Dermer C. D., 2012, *ApJ*, 749, L26
 Baade W., Zwicky F., 1934, *Proceedings of the National Academy of Science*, 20, 259
 Badenes C., Hughes J. P., Bravo E., Langer N., 2007, *ApJ*, 662, 472
 Bamba A., Yamazaki R., Yoshida T., Terasawa T., Koyama K., 2005, *ApJ*, 621, 793
 Baring M. G., Ellison D. C., Reynolds S. P., Grenier I. A., Goret P., 1999, *ApJ*, 513, 311
 Berezhko E. G., Völk H. J., 1997, *Astroparticle Physics*, 7, 183
 Cai Z.-Y., Yang J., Lu D.-R., 2009, *ChAA*, 33, 393
 Cassam-Chenaï G., Hughes J. P., Ballet J., Decourchelle A., 2007, *ApJ*, 665, 315
 Dickel J. R., van Breugel W. J. M., Strom R. G., 1991, *AJ*, 101, 2151
 Dubner G. M., Velázquez P. F., Goss W. M., Holdaway M. A., 2000, *AJ*, 120, 1933
 Foster T., MacWilliams J., 2006, *ApJ*, 644, 214
 Fujita Y., Ohira Y., Tanaka S. J., Takahara F., 2009, *ApJ*, 707, L179
 Gabici S., Casanova S., Aharonian F. A., Rowell G., 2010, in Boissier S., Heydari-Malayeri M., Samadi R., Valls-Gabaud D., eds, *SF2A-2010: Proceedings of the Annual meeting of the French Society of Astronomy and Astrophysics*. p. 313
 Ginzburg V. L., Syrovatskij S. I., 1967, in van Woerden H., ed., *IAU Symposium Vol. 31, Radio Astronomy and the Galactic System*. p. 411
 Giordano F. et al., 2012, *ApJ*, 744, L2
 Giuliani A. et al., 2010, *A&A*, 516, L11
 Gomez H. L. et al., 2012, *MNRAS*, 420, 3557
 Green D. A., 1986, *MNRAS*, 221, 473
 Hayato A. et al., 2010, *ApJ*, 725, 894
 Helder E. A. et al., 2009, *Science*, 325, 719
 Hughes J. P., 2000, *ApJ*, 545, L53
 Hwang U., Decourchelle A., Holt S. S., Petre R., 2002, *ApJ*, 581, 1101
 Inoue T., Yamazaki R., Inutsuka S.-i., Fukui Y., 2012, *ApJ*, 744, 71
 Ishihara D. et al., 2010, *A&A*, 521, L61
 Jiang B., Chen Y., Wang J., Su Y., Zhou X., Safi-Harb S., DeLaney T., 2010, *ApJ*, 712, 1147
 Kang H., Jones T. W., 2006, *Astroparticle Physics*, 25, 246
 Katsuda S., Petre R., Hughes J. P., Hwang U., Yamaguchi H., Hayato A., Mori K., Tsunemi H., 2010, *ApJ*, 709, 1387
 Katz B., Waxman E., 2008, *JCAP*, 1, 18
 Katz-Stone D. M., Kassim N. E., Lazio T. J. W., O'Donnell R., 2000, *ApJ*, 529, 453
 Kelner S. R., Aharonian F. A., Bugayov V. V., 2006, *PRvd*, 74, 034018
 Kirshner R., Winkler P. F., Chevalier R. A., 1987, *ApJ*, 315, L135
 Koo B.-C., Rho J., Reach W. T., Jung J., Mangum J. G., 2001, *ApJ*, 552, 175
 Kothes R., Fedotov K., Foster T. J., Uyaniker B., 2006, *A&A*, 457, 1081
 Krause O., Tanaka M., Usuda T., Hattori T., Goto M., Birkmann S., Nomoto K., 2008, *Nature*, 456, 617
 Lee J.-J., Koo B.-C., Tatematsu K., 2004, *ApJ*, 605, L113
 Lee S.-H., Ellison D. C., Nagasaki S., 2012, *ApJ*, 750, 156
 Li H., Chen Y., 2012, *MNRAS*, 421, 935
 Longair M. S., 1994, *High energy astrophysics. Vol.2: Stars, the galaxy and the interstellar medium*
 Malkov M. A., O'C Drury L., 2001, *Reports on Progress in Physics*, 64, 429
 Moriguchi Y., Tamura K., Tawara Y., Sasago H., Yamaoka K., Onishi T., Fukui Y., 2005, *ApJ*, 631, 947
 Morlino G., Caprioli D., 2012, *A&A*, 538, A81
 Parizot E., Marcowith A., Ballet J., Gallant Y. A., 2006, *A&A*, 453, 387
 Reach W. T., Rho J., 2000, *ApJ*, 544, 843
 Reynoso E. M., Moffett D. A., Goss W. M., Dubner G. M., Dickel J. R., Reynolds S. P., Giacani E. B., 1997, *ApJ*, 491, 816
 Reynoso E. M., Velázquez P. F., Dubner G. M., Goss W. M., 1999, *AJ*, 117, 1827
 Schwarz U. J., Goss W. M., Kalberla P. M., Benaglia P., 1995, *A&A*, 299, 193
 Sgro A. G., 1975, *ApJ*, 197, 621
 Tamagawa T. et al., 2009, *PASJ*, 61, 167
 Tang Y.-Y., Fang J., Zhang L., 2011, *Chinese Physics Letters*, 28, 109501
 Tian W. W., Leahy D. A., 2011, *ApJ*, 729, L15
 Völk H. J., Berezhko E. G., Ksenofontov L. T., 2005, *A&A*, 433, 229
 Warren J. S. et al., 2005, *ApJ*, 634, 376
 Xu J.-L., Wang J.-J., Miller M., 2011, *RAA*, 11, 537
 Zhou P., Chen Y., 2011, *ApJ*, 743, 4
 Zhou X., Chen Y., Su Y., Yang J., 2009, *ApJ*, 691, 516
 Zirakashvili V. N., Aharonian F. A., 2010, *ApJ*, 708, 965